Theor Chem Acc (2009) 123:119–126
DOI 10.1007/s00214-009-0540-1

REGULAR ARTICLE

Influence of the exchange–correlation potential on the description of the molecular mechanism of oxygen dissociation by Au nanoparticles

Alberto Roldán · Josep Manel Ricart · Francesc Illas

Received: 11 February 2009 / Accepted: 11 February 2009 / Published online: 4 March 2009

Abstract The effect of the exchange–correlation functional on the molecular mechanism of dioxygen dissociation by Au nanoparticles is investigated using three Au nanoparticles of increasing size (Au_{25}, Au_{38} and Au_{79}) and various exchange–correlation functionals (local density approach, PW91, PBE and RevPBE. The effect of the exchange–correlation functional on the calculated adsorption energies is quite large and systematic whereas the effect on the calculated energy barriers is much smaller. Implications for the molecular mechanism of O_2 dissociation, involving a competition between desorption and dissociation, are analyzed and discussed in detail.

Keywords Nanogold · Nanocatalysis · DFT · O_2 dissociation

1 Introduction

The discovery that Au nanoparticles with diameter in the range 1–10 nm exhibit unexpected catalytic properties, such as the low temperature oxidation of CO [1–23] has triggered a renewed gold rush [2, 4], but now the chemical activity of this noble element and its possible use in practical applications in the chemical industry being the key question. In fact, the possible use of Au in catalysis is now being actively investigated for both heterogeneously and homogeneously catalyzed reactions [5–7]. For the former, significant advances have been achieved in the recent years for various technologically or environmentally relevant reactions. For instance, one can mention carbon–carbon bond formation and reactions of alkynes and alkenes [8–10], the water gas shift reaction catalyzed by Au supported on ceria [11, 12], the challenging chemoselective reduction of nitro groups on mild conditions catalyzed by Au supported on anatase, which, in addition, provides a route for the synthesis of the industrially relevant cyclohexanone oxime from 1-nitro-1-cyclohexene [13] and selective oxidation of olefins by initiators or oxidant agents such as hydrogen peroxide or adsorbed OOH intermediates [14–16] or, even more recently, directly by dioxygen [17].

The analysis of the existing literature reveals that one of the critical parameters is the small dimension of the gold nanoparticles [5] although support effects have been found to play also a key, and more important than earlier imagined, role [18]. For example, the dissociation of SO_2 on Au nanoparticles supported on TiC(100) takes place readily and the process is more efficient than when the Au nanoparticles are supported on TiO_2(110) and this system is in turn much more efficient than when the support consist of MgO(100) [19]. In a similar way, chemoselective hydrogenation of substituted nitroaromatics implies a subtle interaction between the gold nanoparticles and the support [20] and this can be tuned to transform non selective into chemoselective metal catalysts [21]. From these recent contributions it seems clear that the complexity of gold supported catalysts appears to be higher

Dedicated to Professor Santiago Olivella on the occasion of his 65th birthday and published as part of the Olivella Festschrift Issue.

A. Roldán · F. Illas (✉)
Departament de Química Física i Institut de Química Teòrica i Computacional (IQTCUB), Universitat de Barcelona, C/Martí i Franquès 1, 08028 Barcelona, Spain
e-mail: francesc.illas@ub.edu

A. Roldán · J. M. Ricart
Departament de Química Física i Inorgànica, Universitat Rovira i Virgili, C/Marcel·lí Domingo s/n, 43007 Tarragona, Spain

than imagined, being governed not solely by size effects of the supported gold nanoparticle. Therefore, isolating support from particle effects provides a precise knowledge of the intrinsic reactivity of nanosized gold nanoparticles that it is likely to open a way to improve the properties of gold supported catalysts. For the hydrogenation reactions, the first step implies molecular hydrogen dissociation and it has been recently shown that the necessary and sufficient condition for this process to occur on gold nanoparticles is the presence of low coordinated gold atoms [22]. This conclusion is derived from density functional theory based calculations carried out on a series of Au nanoparticles and of Au stepped surfaces which show that low coordinated Au atoms efficiently split molecular hydrogen without noticeable energy barriers. Here, the need for nanosized nanoparticles seems to be important just to maximize the number of these active sites. The case of selective oxidation reactions catalyzed by gold nanoparticles seems to be more complicated and the particular activity of Au nanoparticles attributed to different origins. Hence, some authors suggested that the enhanced catalytic activity of small Au nanoparticles is due to the increase of low coordinated sites with the decrease of the particle size [23]. However, these conclusions come from the study of stepped surfaces and of a small Au_{10} cluster only [24] or from a rather indirect experimental evidence [25]. Several other authors have also used density functional theory calculations to address the problem of molecular oxygen dissociation by Au nanoparticles but the available information is quite scattered and non systematic. Thus, Wang and Gong [26] found that an icosahedral Au_{32} cluster is able to dissociate molecular oxygen but the dissociation pathway and the corresponding energy barriers were not reported. A more systematic work is reported by Barrio et al. [27] who also found that small Au clusters (Au_{14}, Au_{25} and Au_{28}) activate O_2 but, again, without providing details about the molecular mechanism of O_2 dissociation. In a recent work, Turner et al. [17] have presented strong experimental evidence that Au nanoparticles derived from Au_{55} are able to dissociate molecular oxygen, the first step toward partial oxidation of styrene by dioxygen. However, these authors have also shown that the supported particles are spread in a range of sizes making it difficult to assign the observed catalytic activity to a particular particle or set of particles. Nevertheless, an important conclusion from this work is the firm conclusion that a sharp size threshold exist for the catalytic activity, and that particles with diameters of $\sim$ 2 nm and above are completely inactive.

In a recent work, density functional theory based calculations carried out for a series of models including Au nanoparticles, Au stepped and extended surfaces have lead to the conclusion that the presence of low coordinate Au atoms is not enough to dissociate O_2 and that there is a critical size for Au nanoparticles to dissociate O_2 [28]. These conclusions are based on the computed energy barriers obtained for molecular oxygen dissociation as a function of particle size and taking also into account the desorption energy of the adsorbed molecule. Nevertheless, one must be aware of the fact that these calculations are based on a given approximation to the exact unknown exchange–correlation potential and one may wonder whether the use of a different form for this potential may lead to qualitative changes in the description. For chemical reactions on extended metallic surfaces there is compelling evidence that differences in the adsorption energies, which may be large and are inherent to the use of a different form of the exchange–correlation potential, do not imply noticeable changes in the calculated reaction rates [29–31]. In the present work, we investigate the influence of the exchange–correlation potential on the calculated energy barriers for the dissociation of molecular oxygen on several Au nanoparticles. We will show that, as in the case of extended surfaces [29–31], the adsorption energy depends rather strongly of the particular density functional theory method used. However, this dependence does not largely affect the calculated energy barriers and, as a consequence, previous conclusions about the critical size for molecular oxygen dissociation by Au nanoparticles are further supported.

2 Nanoparticle models and computational details

The effect of the exchange–correlation potential ($E_{xc}[\rho]$) on the description of the molecular mechanism of O_2 dissociation on Au nanoparticles has been studied on Au_{25}, Au_{38} and Au_{79} nanoparticles using periodic density functional theory plane-wave calculations following the procedure previously used in [28]. Single particles have been modeled by placing them in the center of a large enough supercell, with a vacuum space of 1 nm in all directions to avoid interactions between species in the neighboring cells. The use of periodically repeated single particles may seem artificial to readers used to the methods of molecular quantum chemistry but it is a necessary requirement when using a plane-wave basis set, which span the whole space with the periodicity imposed by the chosen unit cell. Nevertheless, this supercell approach has been found to be an efficient way to study the atomic and electronic structure of rather large nanoparticles of coinage metals [32], Pd [33] or of ceria [34–36].

The calculations reported in the present work have been carried out using the VASP code [37, 38] and the total energy has been computed using the local density approach (LDA) to the $E_{xc}[\rho]$ [39], and three different forms of the generalized gradient approach (GGA). These are the

widely used functional due to Perdew and Wang (PW91) [40–42], the so-called PBE functional [43] and the revision of the PBE due to Zhang and Yang [44] hereafter referred to as RevPBE. The PBE functional has been introduced to overcome six shortcomings of the PW91 one and includes an accurate description of the linear response of the uniform electron gas, correct behavior under uniform scaling, a smoother potential and a simpler form. The revision of the PBE exchange–correlation functional by Zhang and Yang intended to improve the PBE atomization energies although Hammer et al. [31] have later shown that this functional also leads to improved adsorption energies of atoms and molecules on transition metal surfaces. Here, it is important to point out that Hammer et al. [31] also proposed a slightly different form of the RevPBE, usually termed RPBE, which provides essentially the same results of the RevPBE but, in addition, fulfills the Lieb-Oxford criterion locally. Despite the fact that PW91 and PBE have different analytical forms, it is commonly assumed that they will produce essentially the same results and, consequently, it is hard to find papers where the two functionals are used and compared. However, there is also increasing evidence that these two functionals are not so equivalent when surface effects are present [45]. This is one of the reasons to investigate their performance in the description of molecular oxygen dissociation catalyzed by Au nanoparticles. The effect of the core electrons on the valence electron density was described by projector augmented wave (PAW) method [46] as implemented by Kresse and Joubert [47] and the cut off for the kinetic energy of the plane-wave basis set has been set to 415 eV, considering only the Γ-point of the reciprocal space. This is a typical value for the cutoff energy and ensures that, for the purposes of the present work, the calculated energies are sufficiently converged [48–50]. Except for the RevPBE functional, total energy calculations were always carried out using the PAW core potentials derived from the $E_{xc}[\rho]$. For the calculations using the RevPBE functional we used the PBE derived PAW potentials. A Gaussian smearing technique with a 0.2-eV width has been applied to enhance convergence but all energies presented below have been obtained by extrapolating to zero smearing (0 K).

The Au_{38} and Au_{79} particles have a cuboctahedral shape and were initially cut from the bulk so as to exhibit low-index planes and their atomic structure fully optimized either in absence or presence of molecular oxygen. The Au_{25} particle is just one half of the Au_{38} unit and is representative of a supported particle. From the various possible ways of molecular adsorption and dissociation on different sites of these particles we have always considered the one which was found to be the minimum energy pathway. This involves the adsorption of the O_2 molecule with the O atoms above bridge sites of a square in an (100) facet and, next, the internuclear distance of the molecule (d_{O-O}) increases in such a way that the final state corresponds to O atoms in threefold hollow sites of the (111) facets (Fig. 1). In order to better understand the effect of particle size on the adsorption energy of O_2, calculations were also carried out for a slab model representing the extended Au(001) surface. The Au(001) slab has been constructed using the lattice parameter corresponding to each functional, it contains four atomic layers interleaved with a vacuum width of 1 nm. The two outermost atomic layers have been always relaxed whereas the other two ones are fixed as in the bulk. For the interaction with O_2, a 5×5 supercell was used resulting in a coverage of atomic oxygen of 0.11. For the slab calculations, a $3 \times 3 \times 1$ grid of Monkhorst–Pack special *k*-points [51] has been used to carry out the integration in the reciprocal space. For such large supercells, this grid of special *k*-points has been found to be dense enough to produce essentially converged relative energies up to 0.01 eV [48, 49]. Except for the isolated O_2 molecule, calculations have been always carried out without spin polarization. Test calculations for a series of structures have proven that for the Au_n nanoparticles and O_2–Au_n complexes spin polarization effects can be neglected.

Transition state (TS) structures were located through the climbing image nudged elastic band (cNEB) method [52–54]. All minima on the potential energy surface were relaxed until self-consistent forces were lower than 0.03 eV/Å and TS structures were fully characterized with the pertinent vibration analysis making sure that TS structures show a single normal mode associated with an imaginary frequency. The calculated vibration frequencies were also used to obtain zero point energy (ZPE) corrections. Consequently, all energies reported in the present work include the ZPE correction. Finally, the rate constant for the O_2 dissociation elementary step (k) has been roughly estimated from the TS theory using the calculated vibrational frequencies of reactants and TS species to

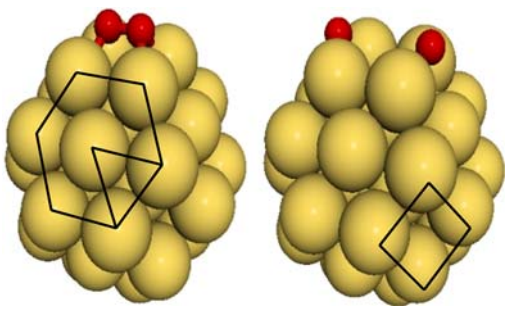

Fig. 1 (*left*) Molecular oxygen adsorbed on Au_{38} (001) facet (*square*) and (*right*) atomic oxygen adsorbed on Au_{38} (111) facets (*hexagon*), respectively

estimate the entropy contribution to the free energy variation in terms of vibrational partition functions [55]. Hence,

$$k = \left(\frac{k_B T}{h}\right)\left(\frac{q^{\#}}{q}\right) e^{-\frac{E_{barr}}{k_B T}} \quad (1)$$

where k_B is the Boltzmann constant, T is the absolute temperature, $q^{\#}$ and q are the vibrational partition functions for the TS and initial state, respectively, and E_{barr} is the activation energy of the elementary step corrected with the ZPE.

3 Results and discussion

In order to facilitate the discussion we will consider first the adsorption energy of the oxygen molecule on each nanoparticle and next we will focus on the calculated energy barriers and their dependence on the exchange–correlation potential. Here, let us just add that the calculated values for the equilibrium internuclear distance of the isolated oxygen molecule (d_{O-O}) predicted by the different exchange–correlation potentials (LDA $d_{O-O} = 1.218$ Å; PW91 $d_{O-O} = 1.235$ Å and PBE or RevPBE $d_{O-O} = 1.244$ Å) is quite close to the experimental value which is 1.207 Å [56].

3.1 Effect of the exchange–correlation potential on the adsorption energy of molecular and atomic oxygen

The adsorption energy of O_2 on each particle has been obtained from the ZPE corrected energy difference between the Au_n nanoparticle and of O_2 at their equilibrium geometry and the minimum energy of the O_2–Au_n complex. Molecular oxygen has been placed above different sites such as corners, edges and surfaces but the best configuration always correspond to adsorption near the four low-coordinate atoms of the (100) facet. In a similar way we also considered the relative stability of two separated atomic oxygen atoms which, as in the case of the Au(111) surface [49], tend to occupy the three hollow sites of the (111) facets. The structures of the adsorbed molecule and of the separated oxygen atoms provide the starting point for the TS search through the cNEB algorithm.

The optimized adsorption geometries of the O_2–Au_n complex do not exhibit significant differences either with respect to the particle size or with respect to functional, d_{O-O} is 1.46 ± 0.02 Å and the nearest Au–O distance (d_{Au-O}) is 2.27 ± 0.07 Å. The noticeable elongation of the O–O distance is a clear indication of bond weakening, whereas the rather short d_{Au-O} distances seem to indicate a rather strong interaction. However, the calculated values of the adsorption energy (E_{ads}) exhibit noticeable differences with both particle size and exchange–correlation potential. For the LDA functional, the calculated E_{ads} value for Au_{79} is very close to that of the Au(001) surface indicating convergence with respect to cluster size. However, this is not the case for the three GGA functionals which all predict E_{ads} values for Au_{79} quite far from the one corresponding to Au(001). Nevertheless, a word of caution is necessary in the view of the positive E_{ads} values predicted by the GGA functionals for Au(001) which indicate that O_2 will not adsorb on this surface.

Next, let us consider the effect of the exchange–correlation functional in some more detail. Table 1 summarizes the E_{ads} values obtained for each particle using the different functionals. In general, the E_{ads} values follow the trend LDA > PW91 > PBE > RevPBE with the LDA values clearly overestimated since they predict quite a strong adsorption of O_2 on Au(001) in clear disagreement with experiment. The interaction of O_2 with the Au_{25}, Au_{38} and Au_{79} nanoparticles follows the trends described by Hammer et al. [31] for the interaction of oxygen, CO and NO with late transition metal surfaces. Table 1 also reports the difference in adsorption energy on going from one functional to the next. Thus ΔLDA is the difference in E_{ads} between LDA and PW91 whereas ΔPW91 is the difference between PBE and PW91 and ΔPBE the difference between RevPBE and PBE. The analysis of Table 1 shows that the differences in E_{ads} between the different functionals seem to follow a systematic trend with $\Delta LDA = 0.75 \pm 0.10$ eV, $\Delta PW91 = 0.18 \pm 0.03$ eV and $\Delta PBE = 0.40 \pm 0.04$ eV. The differences are large enough to lead to qualitative differences regarding the adsorption energy of O_2 on the three nanoparticles, exothermic or endothermic depending on the exchange–correlation potential except for the Au_{38} particle which is predicted to be the one interacting stronger with this molecule. In spite of these important differences, the trend predicted by the different functionals regarding the effect of the particle size is the same, $E_{ads}(Au_{38}) > E_{ads}(Au_{79}) > E_{ads}(Au_{25})$. Strong similarities are also found regarding the charge transfer between the Au nanoparticle and the oxygen molecule which has been estimated using the Bader analysis [57]. The three nanoparticles have core and shell atoms, two shells for Au_{25} and Au_{38} and three for Au_{79}. The Au_{25} particles has five core atoms, four in equatorial plane positive and one near the (001) facet; Au_{38} has six core atoms, four in equatorial plane positive and two perpendiculars to this plane. The interaction with molecular oxygen distorts the Au nanoparticles so that one more shell appears in the radial distribution. Figure 2 (top panel) reports the charge distribution for the Au atoms as a function of the radial distribution. In general, all functionals predict a substantial amount of charge transfer of an approximately −0.9e to the oxygen molecule, the positive

Table 1 Adsorption energy (E_{ads}/eV) for O_2 adsorption on the (001) facets of Au_{25}, Au_{38} and Au_{79} and for LDA, PW91, PBE and RevPBE functional

	E_{ads}/eV			
	LDA	PW91/ΔLDA[a]	PBE/ΔPW91[b]	RevPBE/ΔPBE[c]
Au_{25}	−0.682	0.024/0.706	0.194/0.218	0.576/0.382
Au_{38}	−1.754	−0.906/0.848	−0.719/0.187	−0.278/0.441
Au_{79}	−0.943	−0.191/0.752	0.011/0.202	0.367/0.378
Au(001)	−0.840	0.194/1.034	0.357/0.163	0.805/0.448

Results for the extended Au(001) surface are included for comparison

[a] ΔLDA is the difference in E_{ads} between LDA and PW91

[b] ΔPW91 is the difference between PBE and PW91

[c] ΔPBE is the difference between RevPBE and PBE

charge on the metal atoms tending to accumulate on those close to the oxygen atoms. The charge distribution per atom as a function of radial atomic distance in Fig. 2 also provides information on how each particle modifies his structure upon adsorption, this is clear from the scattering of dots, in the Au_{25} and Au_{38} particles the gold atoms interacting with oxygen increase the gold–gold distances whereas in the Au_{79} particle the atoms interacting with oxygen get closer to the particle core. In all cases, the Au atoms directly interacting with oxygen acquire some positive charge with the missing electron density being donated to the neighboring metallic atoms.

3.2 Effect of the exchange–correlation potential on the energy barrier for O_2 dissociation

Figure 3 displays the energy profile corresponding to the molecular oxygen dissociation pathway as a function of the particle size and for the different exchange–correlation functionals. Let us start the discussion by considering the final state where the two oxygen atoms are well separated. The effect of the exchange–correlation potential on the final state follows almost the same trend described in the previous subsection for the initial state, except for the LDA value for the smallest Au_{25} particle. This is because the presence of adsorbed atomic oxygen has a large effect on the structure of this particle. However, increasing the particles size leads to a considerable decrease in the particle ability to deform and this also influences the $d_{O–O}$ at the TS which decreases with increasing the particle size from $d_{O–O} = 2.02$ Å for Au_{25} to $d_{O–O} = 1.98$ Å and $d_{O–O} = 1.94$ Å, for Au_{38} and Au_{79}, respectively, and for the PW91 functional. The influence of the functional on the TS structure is not very important; LDA gives the smaller $d_{O–O}$ followed by PBE, RevPBE and PW91.

The energy barrier for O_2 dissociation ($\Delta E^{\#}$) is obtained by subtracting the total energy of the Au_n–O_2 complex from the total energy of the TS structure, both corrected by ZPE. From the energy profiles in Fig. 3 and the reported $\Delta E^{\#}$ values we first notice that the PW91 energy barriers are significantly smaller than the one corresponding to the regular Au(111) [50] and the stepped Au(321) surface [58, 59] as expected from the well known different reactivity of Au extended surfaces and Au nanoparticles [1–23]. For the case of H_2 dissociation this difference can be explained in terms of low coordinated sites and, hence, it is predicted that Au(321) will be able to dissociate H_2 with a small energy barrier [22]. This is not the case for the O_2 dissociation where recent work has shown that the existence of these low coordinated sites is not enough to dissociate O_2. Therefore, in the case of O_2 dissociation by Au nanoparticles electronic confinement must play a key role.

The influence of the exchange–correlation potential on the energy barriers is really small, especially for the three GGA functionals. In fact the differences do not exceed 0.04 eV for Au_{25} and Au_{38} and 0.08 eV for Au_{79}. The differences between the three GGA barriers and the LDA one are somehow larger but never exceeding 0.15 eV. This is a very important result since it indicates that, for a given system, the energy barrier does not largely depend on the exchange–correlation potential and hence, the qualitative description of the dissociation process remains essentially unchanged. This conclusion is further confirmed by the calculated values of the rate constants for the dissociation step reported in Table 2. However, one must also realize that molecular oxygen dissociation will only take place when the energy barrier is smaller than the energy required for the molecule to desorb. This is only fulfilled by the Au_{38} particle, in agreement with previous work based on the PW91 only [28], but this conclusion holds also when considering the PW91 and PBE functionals. For the RevPBE, the adsorption energy becomes always too small, especially when compared with the energy barrier for dissociation. Nevertheless, for the Au_{38} particle this energy difference becomes 0.19 eV, well within the error bar for chemisorption energies reported for the RevPBE functional [31], indicating that desorption and dissociation may compete and that the later can be effective when the O_2 pressure is enough to maintain a covered surface. Here, an important question concerns the accuracy of the calculated RevPBE adsorption energies. From the work of Hammer et al. [31] one would expect that the RevPBE values are more accurate although one must also admit that this is based in a rather limited database which does not take into account energy barriers nor does it include calculations for nanoparticles. However, the fact that present values have been obtained using the PBE derived PAW core potentials and the rather large difference between the PBE and RevPBE adsorption energies suggest that the latter are probably underestimated.

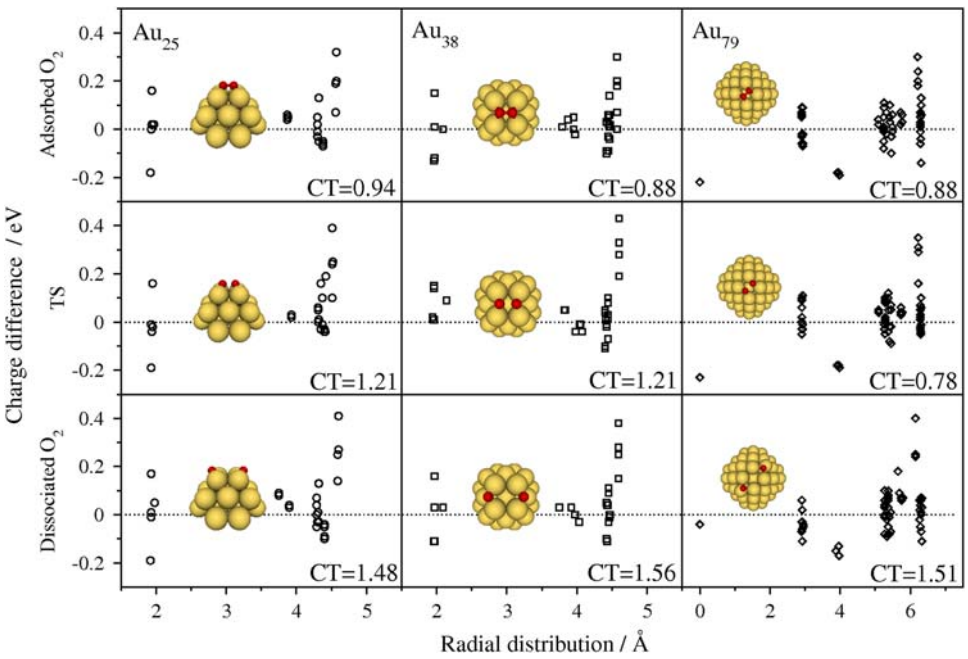

Fig. 2 Atomic charges on Au atoms as a function of radial atomic distribution (in angstrom) for the Au_{25}, Au_{38} and Au_{79} particles obtained from the Bader analysis of the PW91 density functional. The total charge transfer (*CT*) is also shown. The (001) gold atoms interacting with the O_2 molecule are identified with filled points

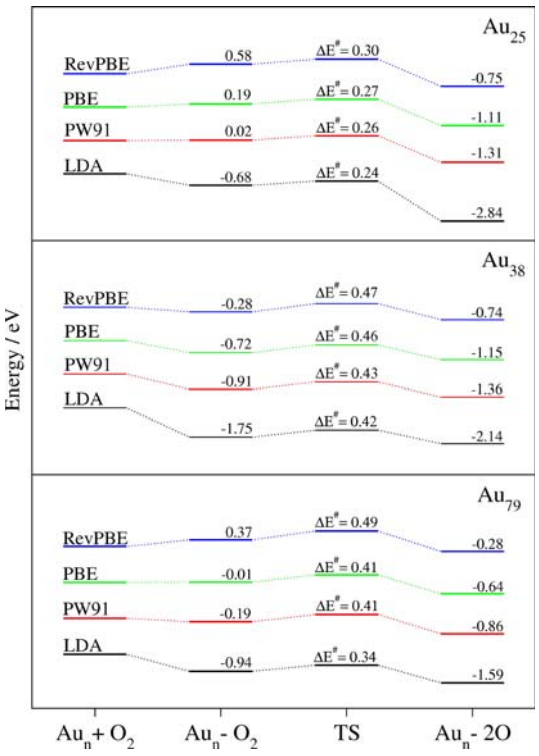

Fig. 3 Profile to dissociate O_2 on the (001) particle facets. Furthermore the effect of exchange–correlation was plotted: LDA, PW91, PBE and RevPBE

To end this discussion we will only add that the dissociation process is accompanied by an increase in the charge transfer from the particle to oxygen molecule as indicated in Fig. 2. Here, the influence of the exchange–correlation functional is less important and will not be further

Table 2 Calculated rate constants for the dissociation step as a function of the particle size and of the exchange–correlation functional

	k/s			
	LDA	PW91	PBE	RevPBE
Au_{25}	3.81×10^8	1.40×10^8	8.94×10^7	3.12×10^7
Au_{38}	4.23×10^5	1.83×10^5	6.97×10^4	2.04×10^4
Au_{79}	1.05×10^7	6.34×10^5	4.54×10^5	1.68×10^4

commented. We will only add that the PW91 charge transfer at the TS is the smallest for Au_{79} which seems to be the reason for the high reaction barrier. In fact, the charge transfer increases from 0.94 and 0.88 e in the adsorbed state for Au_{25} to Au_{38} to 1.21 e at the TS but decreases from 0.88 e in the adsorbed state to 0.78 e at the TS for the Au_{79}. However, the charge transfer at the dissociated state is almost the same ($\sim$1.5 e) for all particles.

4 Conclusions

Density functional calculations carried out for the adsorption and dissociation of molecular oxygen on three Au nanoparticles of modest size (Au_{25}, Au_{38} and Au_{79}) evidences that the adsorption energy is rather strongly dependent on the exchange–correlation functional chosen. The tendency of LDA to strongly overestimate the adsorption energy reported by various authors [60–64] is confirmed for the case of O_2 adsorption on Au nanoparticles. The difference between the predictions of the three GGA functionals is smaller than from these to GGA but

noticeable, the PW91 values being larger than the PBE by roughly 0.20 eV and those are larger than the RevPBE by about 0.35 eV. The deviations are found to be systematic and, hence, the main trends remain unaltered. The influence of the exchange–correlation functional on the energy barriers for O_2 dissociations are, however, much smaller. On the one hand this is a good new since it indicates that, for a given system, the description of this elementary step does not depend on the choice of the functional. On the other hand, this different behavior of chemisorption energies and energy barriers with respect to the exchange–correlation functional has some undesirable effects, especially when the competition between adsorption and dissociation becomes crucial as is the case here for O_2 dissociation on Au nanoparticles. Nevertheless, the calculated results confirm previous work indicating that there is a critical size for the Au nanoparticles to efficiently dissociate O_2 [28]. In fact, PW91 and PBE calculations show that Au_{38} is the only particle where O_2 dissociation clearly dominates over O_2 dissociation whereas RevPBE calculations point to a less clear trend although still indicating that dissociation may occur. This is not the case for the other two Au nanoparticles where all functionals predict that desorption will always take place.

Finally, the present calculations provide theoretical support to recent experimental work indicating that direct styrene epoxidation by dioxygen requires really small particles [17], reinforces previous theoretical findings [29] and is in agreement with the even more recent experimental work of Hutchings and colleagues [65] showing that subnanometer Au particles supported on FeO_x are active for CO oxidation.

Acknowledgments Alberto Roldán thanks Universitat Rovira i Virgili, for supporting his pre-doctoral research. Financial support has been provided by the Spanish Ministry of Science and Innovation (MICINN) (grants FIS2008-02238/FIS and CTQ2008-06549-C02-01) and, in part, by the Generalitat de Catalunya (Grants 2005SGR00697, 2005SGR-00104 and 2005 PEIR 0051/69). Computational time on the Marenostrum supercomputer of the Barcelona Supercomputing Center is gratefully acknowledged.

References

1. Haruta M (1997) Catal Today 36:153–166. doi:10.1016/S0920-5861(96)00208-8
2. Haruta M (2005) Nature 437:1098–1099
3. Valden M, Lai X, Goodman DW (1998) Science 281:1647–1650. doi:10.1126/science.281.5383.1647
4. Nolan SP (2007) Nature 445:496–497. doi:10.1038/445496a
5. Hashmi ASK (2007) Chem Rev 107:3180–3211. doi:10.1021/cr000436x
6. Hashmi ASK, Hutchings GJ (2006) Angew Chem Int Ed Engl 45:7896–7936
7. See also the reviews in the special issue dedicated to chemistry of nano-gold in (2008) Chem Soc Rev 37
8. Carrettin S, Guzman J, Corma A (2005) Angew Chem Int Ed Engl 44:2242–2245. doi:10.1002/anie.200462560
9. González-Arellano C, Corma A, Iglesias M, Sánchez F (2006) J Catal 238:497–501
10. González-Arellano C, Abad A, Corma A, García H, Iglesias M, Sánchez F (2007) Angew Chem Int Ed Engl 119:1558–1560. doi:10.1002/ange.200604746
11. Fu Q, Weber A, Flytzani-Stephanopoulos M (2003) Science 301:935–938. doi:10.1126/science.1085721
12. Rodriguez JA, Ma S, Liu P, Hrbek J, Evans J, Perez M (2007) Science 318:1757–1760. doi:10.1126/science.1150038
13. Corma A, Serna P (2006) Science 313:332–334. doi:10.1126/science.1128383
14. Hughes MD, Xu YJ, Jenkins P, McMorn P, Landon P, Enache DI, Carley AF, Attard GA, Hutchings GJ, King F, Stitt EH, Johnston P, Griffin K, Kiely CJ (2005) Nature 437:1132–1135. doi:10.1038/nature04190
15. Nijhuis TA, Weckhuysen BM (2006) Catal Today 117:84–89
16. Chowdhury B, Bravo-Suarez JJ, Mimura N, Lu J, Bando KK, Tsubota S, Haruta M (2006) J Phys Chem B 110:22995–22999. doi:10.1021/jp066008y
17. Turner M, Golovko VB, Vaughan OPH, Abdulkin P, Berenguer-Murcia A, Tikhov MS, Johnson BFG, Lambert RM (2008) Nature 454:981–983. doi:10.1038/nature07194
18. Corma A, Garcia H (2008) Chem Soc Rev 37:2096–2126. doi:10.1039/b707314n
19. Rodriguez JA, Liu P, Viñes F, Illas F, Takahashi Y, Nakamura K (2008) Angew Chem Int Ed Engl 47:6685–6689. doi:10.1002/anie.200801027
20. Boronat M, Concepción P, Corma A, González S, Illas F, Serna P (2007) J Am Chem Soc 129:16230–16237. doi:10.1021/ja076721g
21. Corma A, Serna P, Concepción P, Calvino JJ (2008) J Am Chem Soc 130:8748–8753. doi:10.1021/ja800959g
22. Corma A, Boronat M, Gonzalez S, Illas F (2007) Chem Commun 3371–3373
23. Lopez N, Janssens TVW, Clausen BS, Xu Y, Mavrikakis M, Bligaard T, Nørskov JK (2004) J Catal 223:232–235. doi:10.1016/j.jcat.2004.01.001
24. Remediakis IN, Lopez N, Nørskov JK (2005) Angew Chem Int Ed Engl 44:1824–1826. doi:10.1002/anie.200461699
25. Deng X, Min BK, Guloy A, Friend CM (2005) J Am Chem Soc 127:9267–9270. doi:10.1021/ja050144j
26. Wang Y, Gong X (2006) J Chem Phys 125(1–12):124703
27. Barrio L, Liu P, Rodriguez JA, Campos-Martin JM, Fierro JLG (2007) J Phys Chem C 111:19001–19008. doi:10.1021/jp073552d
28. Roldán A, González S, Ricart JM, Illas F (2009) Chem Phys Chem 10:348–351. doi:10.1002/cphc.200800702
29. Honkala K, Hellman A, Remediakis IN, Logadottir A, Carlsson A, Dahl S, Christensen SH, Nørskov JK (2005) Science 307:555–558. doi:10.1126/science.1106435
30. Strasser P, Fan Q, Devenney M, Weinberg WH, Liu P, Nørskov JK (2003) J Phys Chem B 107:11013–11021
31. Hammer B, Hansen LB, Nørskov JK (1999) Phys Rev B 59:7413–7421. doi:10.1103/PhysRevB.59.7413
32. Roldan A, Vines F, Illas F, Ricart JM, Neyman KM (2008) Theor Chem Acc 120:565–573. doi:10.1007/s00214-008-0423-x
33. Viñes F, Illas F, Neyman KM (2008) J Phys Chem A 112:8911–8915. doi:10.1021/jp8014854
34. Loschen C, Bromley S, Neyman KM, Illas F (2007) J Phys Chem C 111:10142–10145. doi:10.1021/jp072787m
35. Migani A, Loschen C, Illas F, Neyman KM (2008) Chem Phys Lett 465:106–109
36. Loschen C, Migani A, Bromley ST, Illas F, Neyman KM (2008) Phys Chem Chem Phys 10:5730–5738. doi:10.1039/b805904g
37. Kresse G, Furthmuller J (1996) Comput Mater Sci 6:15–50. doi:10.1016/0927-0256(96)00008-0

38. Kresse G, Furthmueller J (1996) Phys Rev B 54:11169–11186. doi:10.1103/PhysRevB.54.11169
39. Vosko SH, Wilk L, Nusair M (1980) Can J Phys 58:1200–1211
40. Perdew JP, Chevary JA, Vosko SH, Jackson KA, Pederson MR, Singh DJ, Fiolhais C (1992) Phys Rev B 46:6671–6687. doi:10.1103/PhysRevB.46.6671
41. Perdew JP, Chevary JA, Vosko SH, Jackson KA, Pederson MR, Singh DJ, Fiolhais C (1993) Phys Rev B 48:4978–4978
42. Perdew JP, Wang Y (1992) Phys Rev B 45:13244–13249. doi:10.1103/PhysRevB.45.13244
43. Perdew JP, Burke K, Ernzerhof M (1997) Phys Rev Lett 78:1396–1399. doi:10.1103/PhysRevLett.78.1396
44. Zhang Y, Yang W (1998) Phys Rev Lett 80:890. doi:10.1103/PhysRevLett.80.890
45. Mattsson AE, Armiento R, Schultz PA, Mattsson TR (2006) Phys Rev B 73(1–7):195123
46. Blöchl PE (1994) Phys Rev B 50:17953–17979. doi:10.1103/PhysRevB.50.17953
47. Kresse G, Joubert D (1999) Phys Rev B 59:1758–1775. doi:10.1103/PhysRevB.59.1758
48. Torres D, Lopez N, Illas F (2006) J Catal 243:404–409. doi:10.1016/j.jcat.2006.08.011
49. Torres D, Neyman KM, Illas F (2006) Chem Phys Lett 429:86–90
50. Torres D, Illas F (2006) J Phys Chem B 110:13310–13313. doi:10.1021/jp0625917
51. Monkhorst HJ, Pack JD (1976) Phys Rev B 13:5188–5192. doi:10.1103/PhysRevB.13.5188
52. Henkelman G, Jonsson H (2000) J Chem Phys 113:9978–9985. doi:10.1063/1.1323224
53. Henkelman G, Uberuaga BP, Jonsson H (2000) J Chem Phys 113:9901–9904
54. Henkelman G, Jonsson H (1999) J Chem Phys 111:7010–7022. doi:10.1063/1.480097
55. Laidler KJ (1987) Chemical kinetics, 3rd edn. Harper Collins, New York
56. Huber KP, Herzberg G (1979) Molecular spectra and molecular structure IV. Constants of diatomic molecules, Van Nostrand Reinhold, New York
57. Sanville E, Kenny SD, Smith R, Henkelman G (2007) J Comput Chem 28:899–908. doi:10.1002/jcc.20575
58. Fajin JLC, Cordeiro MNDS, Gomes JRB (2007) J Phys Chem C 111:17311–17321. doi:10.1021/jp073796y
59. Fajin JLC, Cordeiro MNDS, Gomes JRB (2008) J Phys Chem C 112:17291–17302. doi:10.1021/jp8031435
60. White JA, Bird DM, Payne MC, Stich I (1994) Phys Rev Lett 73:1404–1407. doi:10.1103/PhysRevLett.73.1404
61. Hammer B, Jacobsen KW, Nørskov JK (1993) Phys Rev Lett 70:3971–3974
62. Hu P, King DA, Crampin S, Lee MH, Payne MC (1994) Chem Phys Lett 230:501–506
63. Philipsen PHT, te Velde G, Baerends EJ (1994) Chem Phys Lett 226:583–588
64. Hammer B, Scheffler M, Jacobsen KW, Nørskov JK (1994) Phys Rev Lett 73:1400–1403. doi:10.1103/PhysRevLett.73.1400
65. Herzing AA, Kiely CJ, Carley AF, Landon P, Hutchings GJ (2008) Science 321:1331–1335. doi:10.1126/science.1159639